

AD-A213 169

Unclassified
SECURITY CLASSIFICATION OF THIS PAGE

REPORT DOCUMENTATION PAGE				Form Approved OMB No. 0704-0188	
1a. REPORT SECURITY CLASSIFICATION Unclassified			1b. RESTRICTIVE MARKINGS		
2a. SECURITY CLASSIFICATION AUTHORITY			3. DISTRIBUTION / AVAILABILITY OF REPORT		
2b. DECLASSIFICATION / DOWNGRADING SCHEDULE			Distribution Unlimited		
4. PERFORMING ORGANIZATION REPORT NUMBER(S) FINAL			5. MONITORING ORGANIZATION REPORT NUMBER(S)		
6a. NAME OF PERFORMING ORGANIZATION SRI International		6b. OFFICE SYMBOL (If applicable)		7a. NAME OF MONITORING ORGANIZATION Defense Logistics Agency DCASMA San Francisco	
6c. ADDRESS (City, State, and ZIP Code) 333 Ravenswood Avenue Menlo Park, CA 94025		7b. ADDRESS (City, State, and ZIP Code) 1250 Bayhill Drive San Bruno, CA 94066			
8a. NAME OF FUNDING / SPONSORING ORGANIZATION Office of Naval Research		8b. OFFICE SYMBOL (If applicable)		9. PROCUREMENT INSTRUMENT IDENTIFICATION NUMBER N0014-86-C-0121	
8c. ADDRESS (City, State, and ZIP Code) 800 North Quincy Street Arlington, VA 22217		10. SOURCE OF FUNDING NUMBERS			
		PROGRAM ELEMENT NO.		PROJECT NO.	
		TASK NO.		WORK UNIT ACCESSION NO.	
11. TITLE (Include Security Classification) MECHANISMS OF CO ₂ REDUCTION METAL AND METAL MODIFIED SEMICONDUCTOR ELECTRODES					
12. PERSONAL AUTHOR(S) K. W. Frese, Jr.					
13a. TYPE OF REPORT FINAL		13b. TIME COVERED FROM 12/85 TO 12/88		14. DATE OF REPORT (Year, Month, Day) September 20, 1989	
15. PAGE COUNT 9					
16. SUPPLEMENTARY NOTATION					
17. COSATI CODES			18. SUBJECT TERMS (Continue on reverse if necessary and identify by block number)		
FIELD	GROUP	SUB-GROUP			
19. ABSTRACT (Continue on reverse if necessary and identify by block number) Fundamental studies were made to elucidate the factors that control the rate of electrochemical reduction of carbon dioxide. The reorganization energies for CO ₂ and H ⁺ reduction were 3.1 and 1.95 eV, respectively. Models were developed that allow prediction of binding energies of adsorbed intermediates on electrode surfaces. Pd, Mo, and GaAs (111) were found to be among the best materials that catalyzed the reduction of CO ₂ to CH ₃ OH. (A10)					
20. DISTRIBUTION / AVAILABILITY OF ABSTRACT <input checked="" type="checkbox"/> UNCLASSIFIED/UNLIMITED <input type="checkbox"/> SAME AS RPT <input type="checkbox"/> DTIC USERS			21. ABSTRACT SECURITY CLASSIFICATION		
22a. NAME OF RESPONSIBLE INDIVIDUAL Dr. H. E. Guard. ONR			22b. TELEPHONE (Include Area Code) 202-696-4409		22c. OFFICE SYMBOL

OFFICE OF NAVAL RESEARCH

FINAL REPORT
September 20, 1989

for
Contract N0014-86-C-0121

R & T Code 413-G-007

Mechanisms of CO₂ Reduction on Metal and Metal-modified Semiconductor Electrodes.

Principle Investigator: K. W. Frese, Jr.
SRI International
Menlo Park, Ca. 94025

Reproduction in whole or in part is permitted for any purpose of the United States Government.
This document has been approved for public release and sale; its distribution is unlimited.



September 20, 1989

Final Report

For the Period December 30, 1986, to January 1, 1989

MECHANISMS OF CO₂ REDUCTION ON METAL AND METAL MODIFIED SEMICONDUCTOR ELECTRODES

By: K. W. Frese, Jr.

Prepared for:

OFFICE OF NAVAL RESEARCH

Attn: Dr. Harold E. Guard

ONR Contract No. Contract N0014-86-C-0121

SRI Project PYU 1635

D. D. Macdonald, Laboratory Director
Materials Research Laboratory

G. R. Abrahamson
Vice President
Physical Sciences Division



Accession For	
NTIS	<input checked="" type="checkbox"/>
DTIC	<input type="checkbox"/>
Unpublished	<input type="checkbox"/>
Justification	
By	
Distribution/	
Availability Codes	
Dist	Special
A-1	

PART I

Papers Published with ONR Support During the Annual Report Period

1. Calculation of Gibbs Free Energies of Hydration With the Ion-Dielectric Sphere Model J. Phys. Chem., 93, 591 (1989).
2. Application of the Sanderson Polar Covalence Model to Energetics of CO Adsorption, Surf. Sci., 202, 277 (1988).
3. The Reorganization Energy of the Aqueous Proton, J. Electroanalytical Chem., 249, 15 (1988).
4. Calculation of Surface Binding Energies for Hydrogen, Oxygen, and Carbon Atoms, 182, 85 (1987).
5. Electrochemical Reduction of CO₂ and CO at Cu Electrodes. J. Electroanalytical Chem., 245, 223 (1988). Partial Support by the Gas Research Institute.

Other Related Publications During the Annual Report Period

6. The Electrochemical Reduction of Aqueous Carbon Monoxide and Methanol to Methane at Ruthenium Electrodes. J. Electrochem. Soc., 135, 265 (1988).
7. Electrochemical Reduction of Carbon Dioxide. Characterization of the Formation of Methane at Ru Electrode., Langmuir, 4, 51 (1988).
8. Mechanistic Aspects of the Electrochemical Reduction of CO and CH₃OH to CH₄ at Ru and Cu Electrodes, Electrochemical Surface Science. Molecular Phenomena at Electrode Surfaces, ACS Symposium 378, M. P. Soriaga (ed.), New Orleans. The American Chemical Society Wash., DC 1988.

9. Electrochemical Reduction of Aqueous Carbon Dioxide at Electroplated Ru electrodes, Investigations towards the Mechanism of CH₄ Formation. Catalytic Activation Of Carbon Dioxide ACS Symposium 363 , W. M. Ayers (ed.), New York. The American Chemical Society Wash., DC 1988.

Book Chapters During the Annual Report Period

1. Gallium Arsenide in Semiconductor Electrodes, H. O. Finklea (ed.). Studies in Physical and Theoretical Chemistry Series No. 55. K. W. Frese, Jr. Elsevier, Amsterdam (1988).
2. In Preparation. Electrochemical Reduction of CO₂ on Solid Electrodes in Electrochemical and Electrocatalytic Reduction of Carbon Dioxide, Elsevier Publishing Co.

Invited Papers During the Annual Report Period

1. Electrochemical Reduction of CO₂ and CO at Cu Electrodes. K. W. Frese, J.J. Kim and D. P. Summers. Paper presented at the Electrochemical Society Fall Meeting, Honolulu, Hawaii, Abstract 833. October 1987.
2. CO₂ Reduction at Single Crystal and Polycrystalline Cu Electrodes. Lecture at the National Science Foundation Joint U.S - Japan Conference on Photoelectrochemical Synthesis. K.W. Frese. Gleneden Beach, Oregon. June 1988.
3. Mechanistic Aspects of the Electrochemical Reduction of CO₂, CO, and CH₃OH to CH₄ at Ru Electrodes. D. P. Summers and K. W. Frese, Jr., 194 ACS Meeting, August 1987, New Orleans. (Partial GRI Support).
4. Photooxidation of CH₄ at Semiconductor-Granular Metal Electrodes. Abstract 362 . Symposium on Semiconductor Electrolyte Interfaces The 175th Meeting of the Electrochemical Society , Los Angeles, May 1989.

Workshops

SRI hosted a three day Carbon Dioxide Workshop sponsored by the Office of Naval Research, April 1988.

PART II

Principle Investigator
Cognizant ONR Scientific Officer
Telephone No.

Dr. Karl W. Frese, Jr.
Dr. Harold Guard
415-859 3221

Project Description

The goal of this project is to gain an understanding of the factors that control the rate of electrochemical reduction of CO₂ with particular emphasis on the formation of methanol. The approach combines theoretical calculations with kinetic measurements on various metal and semiconductor surfaces. The theoretical calculations of surface thermodynamics are helpful in identifying allowed elementary steps and ruling out steps that are thermodynamically difficult. Mechanistic determinations are aided by estimates of rate constants for elementary steps. Therefore we are exploring methods of calculating rate constants for elementary steps in the CO₂ reduction pathway. Laboratory experiments include electrolysis of CO₂ saturated electrolytes and analysis of product distributions as a function of electrode identity, surface preparation, electrode potential, temperature, and pH.

Significant Results

As part of the investigation of rate constants of elementary steps, we considered the addition of an electron to the CO₂ molecule in an electrolyte. The activation energy for the uncatalyzed process is determined by the reorganization energy of the molecule. Two methods were used to obtain the reorganization energy. The Marcus equation was used to analyze the ab-initio energy surfaces for the gaseous CO₂/CO₂⁻ couple. This gives the inner reorganization energy of 2.5 eV, a large value. The electrostatic contribution was found to be 0.6 eV by means of the Marcus equations. The total reorganization energy was found to be about 3.1 eV. The major reason for the relatively slow kinetics has been found to be the bending of the CO₂ bond angle from 180 to 149° in the transition

state. Analysis of exchange current density data for CO₂ reduction to formate (limited by electron addition to CO₂) yielded 3.2 eV for the total reorganization energy.

The Sanderson model of Polar Covalence was proven to be useful for the calculation of the energetics of CO adsorption on fifteen metals. The heats of adsorption of various stereochemical forms including linear, bridged and dissociated CO were successfully calculated. The data were compared with a combination of HREELS, LEED and thermal desorption data from the literature. Average deviation of the calculated results from the experimental values was about 2-3 kcal mol⁻¹. These results coupled with successful calculations of binding energies of H, C and O atoms gives us confidence that we can calculate the energetics of surface reactions involving bond with transition metals and the just mentioned atoms.

We also developed a useful method for predicting the bond length of adsorbed CO molecules on metal surfaces. The method is based on quantum mechanics and utilizes the partial charges on bonded atoms determined by the Sanderson method. These theoretical data were needed in the above calculations of CO binding. We believe they are accurate to 0.005 Å.

The rate of CO₂ reduction to CH₄, CO and H₂ was studied on Cu single crystal electrodes in KHCO₃ solution. The results showed that the (111) plane has the highest methane formation rate. The (100) has the lowest, with (110) intermediate. This is the first evidence that crystal plane effects exist for CO₂ reduction on metal, as opposed to semiconductor, surfaces. The relative rates correlated with the heat of adsorption of CO. The CO is bound weakest on (111) and strongest on (100). CO has been shown to be an important intermediate in the CO₂ to CH₄ pathway.

Table 1 summarizes results on the rates of formation of methanol on various electrode surfaces in aqueous CO₂ saturated electrolytes. Among the metals, Mo and Pd electrode gave the highest rates of methanol formation, and GaAs (111) the highest of the semiconductors tested.

Table 1
Materials for CO₂ to CH₃OH Conversion

METAL	ELECT.	V(SCE)	^a RATE	F
GaAs(As111)	Na ₂ SO ₄	-1.2 to -1.4	6 x 10 ⁻⁷	100
(100)				0
(110)				0
InP(P111)	Na ₂ SO ₄	-1.2 to -1.4	3.7 x 10 ⁻⁷	80
Mo	Na ₂ SO ₄	-0.8	5.0 x 10 ⁻⁷	80
Mo(cycled)	Na ₂ SO ₄	-0.8	1.6 x 10 ⁻⁶	300
Au	KHCO ₃	-1.2	4.8 x 10 ⁻⁷	38
Ag on Cu	KHCO ₃	-1.35	2.6 x 10 ⁻⁶	63
Re	KHCO ₃	-1.20	1.9 x 10 ⁻⁶	15
10% Ru/Pt	KHCO ₃	-1.20	7.1 x 10 ⁻⁷	9
Cu(60 °C)	Na ₂ SO ₄	-1.30	2.0 x 10 ⁻⁶	19
Zn	Na ₂ SO ₄	-1.20	9.7 x 10 ⁻⁷	39
Pd	KHCO ₃	-1.10	1.8 x 10 ⁻⁶	59

a. mol cm⁻²hr⁻¹, F = faradaic efficiency

Future Plans

During the coming year, we will concentrate on three areas. We will continue to evaluate the thermodynamics of all conceivable elementary steps in the CO₂ reduction pathway on various metal surfaces. The goal will be to determine the most likely steps and suggest how they may vary on different metals.

The results of the surface thermodynamic study will guide us towards the realization of an effective catalyst for methanol formation. Electrodes consisting of Cu/Zn and CuO/ZnO will be investigated for catalytic activity for methanol formation.

We will apply our open circuit transient technique and ac impedance methods to investigate overpotential deposited intermediates on electrode surfaces undergoing CO₂ reduction. This information is necessary for the elucidation of reaction intermediates.

We have received a renewal contract, extending the work for another 18 months. During this time we will focus on the role of oxides and composite surfaces in CO₂ reduction. For example, in the renewal proposal, we suggested a strategy for ethylene glycol formation on Cu/Ag electrodes. This approach utilizes the special chemistry at Cu to form ethylene from CO₂ and oxygen bearing silver to catalyze epoxidation of ethylene.

Technical Reports

A copy of the published version of technical report No 5 (ref 1 above) is attached.

Personnel

Drs. J. J. Kim and Mr. Mike Cinnibulk also contributed to the ONR program.

Calculation of Gibbs Hydration Energy with the Ion-Dielectric Sphere Model

Karl W. Frese, Jr.

Materials Research Laboratory, SRI International, Menlo Park, California 94025
(Received: December 17, 1987; In Final Form: March 7, 1989)

The Gibbs energy of hydration of gaseous ions of -1 to $+4$ charge is calculated on the basis of the exact electrostatic solution for the interaction energy of an ion and groups of dielectric spheres. Dispersion energies were added. The average error of the method is 2%. The dielectric constant of the spheres is assumed to be described by Booth's field-dependent version of Kirkwood's theory. The energetic contributions of successive layers of water are obtained by demanding a self-consistent dielectric constant at each shell of water. The results confirm that 78–90% of the hydration energy, depending on the ion, involves water in the inner layer. The accuracy of the Born expression for solvated complex ions, $M(H_2O)_n^{+/-}$, is in doubt. Inner-layer hydration numbers ranging from 4 to 12 were obtained.

Introduction

Model calculation of the Gibbs energy of hydration of gaseous ions, ΔG_{hyd} , has a long history.¹ Experimentally derived values^{2–6} have been tabulated. The subject has been reviewed by Case,⁴ Friedman, and Krishnan,⁵ and Conway.⁷ Survey of this work shows that no one model has been used successfully to calculate ΔG_{hyd} for ions with -2 to $+4$ charges. Most authors have limited their comparisons between theory and experiment to univalent species. For example, many calculations^{8–11} for single-charge species such as Na^+ and Cl^- ions have been made with good results. These same model calculations, some of which utilize the Born model outside the primary hydration layer in the form of eq 1a,

$$\Delta G_{\text{BC}} = -\frac{(ze_0)^2}{2(r_i + r_w)} \left(1 - \frac{1}{\epsilon}\right) \quad (1a)$$

are usually not applied to higher charged species. The simple Born model with $r_w = 0$ is known to fail for both small and highly charged ions. Replacement of r_w with empirical values³ characteristic of univalent anions and cations reduces the errors to about 10% for Fe^{2+} and Fe^{3+} . Although the Born model is accepted as reliable for the hydration energy of the complex ion composed of a univalent ion and its primary hydration layer, it is not clear that such a model would be accurate for $+2$, $+3$, or $+4$ complex ions. Furthermore, the electrostatic model treatments of the inner layer of hydration may be improved. We attempt to show below, with improved models of the inner-layer hydration, that eq 1a is not accurate beyond the first shell of water.

A number of studies are based on combination of eq 1a with the dipole and quadrupole moment interaction expressions. The model of Buckingham,⁸ for example, makes use of ion-dipole, eq 1b, ion-induced-dipole, eq 1c, and ion-quadrupole terms.

$$\Delta G_{\text{I-D}} = -N \frac{(ze_0)\mu_w}{(r_i + r_w)^2} \quad (1b)$$

$$\Delta G_{\text{I-ID}} = -N \frac{\alpha(ze_0)^2}{2(r_i + r_w)^4} \quad (1c)$$

Muirhead-Gould and Laidler,¹² who did attempt calculations for -1 to $+4$ ions, also included questionable ion-induced-dipole terms. Generally, ion-dipole and ion-induced-dipole terms are calculated to be large energies. The former has been reported^{8,10} to be of the order of the heat of hydration. Bottcher¹³ in 1952 stated that simple expressions such as eq 1b,c are not accurate at ordinary bond distances of 2–3 Å in the inner hydration layer. He showed that errors of 50–100% are expected. Yet these expressions were used repeatedly in subsequent years. At bond distances, the r^{-1} term of the Born model is an overestimation, and the r^{-2} and r^{-4} terms are underestimations of the true energy at a given distance.

In addition, the quadrupole moment used in the Buckingham model is about an order of magnitude smaller^{4,14} than the measured value for water. In the series of positive ions Li^+ , Na^+ , K^+ , Rb^+ , and Cs^+ , the magnitude of calculated¹⁰ ion-quadrupole energy varies from 53 to 26% of the total hydration energy. If these values are revised downward an order of magnitude, the agreement with experiment would be much worsened. As an additional example of the failure of the model described by Buckingham, consider the Fe^{2+} ion. The calculated heat of hydration is $-676 \text{ kcal mol}^{-1}$ compared to the experimentally derived value^{2,5} of $-480 \text{ kcal mol}^{-1}$, an error of about 40%. Larger errors would be obtained for higher charges and for smaller ions of similar charge and a more realistic quadrupole moment.

In this paper we present an improved electrostatic model of ion-solvent interactions that is able to reproduce the hydration free energies of ions with any charge type -1 to $+4$ with an average error of 2.1%. The ion-dipole, ion-induced-dipole, and ion-quadrupole terms do not appear explicitly in the energy expression. The contribution of each shell of solvent to the total hydration energy is obtained. The equations are based on the exact electrostatic solution¹⁵ to the problem of the interaction energy of a charged particle with a neighboring dielectric sphere. The dielectric constant, ϵ , of the spheres depends on the electric field at their respective positions. The use of the dielectric properties of the medium is analogous to the dielectric function approach¹⁵ used by physicists in the theories on interaction of ions and electrons in metals. Quantum mechanical dispersion energies¹⁶

- (1) Marcus, Y. *Ion Solvation*; Wiley: Chichester, 1985.
- (2) Noyes, R. M. *J. Am. Chem. Soc.* **1962**, *84*, 513.
- (3) Rosseinsky, D. R. *Chem. Rev.* **1965**, *65*, 467.
- (4) Case, B. *Reaction of Molecules at Electrodes*; Hush, N. S., Ed.; Wiley: New York, 1971.
- (5) Friedman, H. L.; Krishnan, C. V. *Water: A Comprehensive Treatise*; Franks, F., Ed.; Plenum Press: New York, 1973; Vol. 3.
- (6) Notoya, R.; Matsuda, A. *J. Res. Catal., Hokkaido Univ.* **1982**, *30*, 61.
- (7) Conway, B. E. *Ionic Hydration in Chemistry and Physics*; Elsevier: Amsterdam, 1981.
- (8) Buckingham, A. D. *Discuss. Faraday Soc.* **1957**, *24*, 151.
- (9) Gluckauf, E. *Chemical Physics of Ionic Solutions*; Conway, B. E., Barradas, R. G., Eds.; Wiley: New York, 1965; p 67.
- (10) Bockris, J. O'M.; Saluja, P. P. *J. Phys. Chem.* **1972**, *76*, 2298.
- (11) Abraham, M. H.; Lisiz, J. *J. Chem. Soc., Faraday Trans. 1* **1978**, *74*, 1604.

- (12) Muirhead-Gould, J. S.; Laidler, K. J. *Chemical Physics of Ionic Solutions*; Conway, B. E., Barradas, R. G., Eds.; Wiley: New York, 1965; p 75.
- (13) Bottcher, C. J. F. *Theory of Electric Polarization*; Elsevier: Amsterdam, 1952; Chapter 5.
- (14) Kistenmacher, H.; Popkie, H.; Clementi, E. *J. Chem. Phys.* **1974**, *61*, 799.
- (15) Harrison, W. A. *Electronic Structure and the Properties of Solids*; W. H. Freeman: San Francisco, 1980.
- (16) Pitzer, K. S. *Advances in Chemical Physics*; Prigogine, I., Ed.; Interscience: New York, 1959; Vol. 11, p 69.

are added to the electrostatic results to give the chemical part of the hydration free energy. Bucher and Porter¹⁷ have determined nonelectrostatic short-range interaction energies by subtracting an electrostatic contribution from the observed Gibbs energy of hydration. The much smaller energy associated with the transfer of the ion across the vacuum-solvent interface⁵ was not considered in the present work and poses no special problem because experimentally derived free energies of hydration do not include this quantity.

Our motivation for this work is related to an important question in electrochemistry concerning the role of solvent molecules held on a charged electrode. It is generally assumed, following the detailed calculation of Bockris and Hill¹⁸ on Hg electrodes, that a monolayer of solvent covers the electrode. This means that elementary steps in certain electrochemical mechanisms should be considered as solvent displacement reactions¹⁹ and therefore the binding energy of the solvent becomes an important consideration. Before attempting a calculation of solvent binding on electrodes, we thought it necessary to seek improved methods of calculation of the energetics of electrostatic binding of water to both ions and, by analogy, charged electrode surfaces.

Theory

Synthesis of an Electrostatic Model for $\Delta G_{\text{hyd}}(\text{el})$. The BASIC computer program we developed for the electrostatic contribution to ΔG_{hyd} is based upon an equation from Bottcher¹³ that quantifies the interaction energy between an ion of charge q and a neighbor spherical region or regions of dielectric constant, ϵ . The term W below represents the electrostatic free energy change¹³ for the process in which the ion and sphere are brought together from infinite separation. In our calculations the neighboring spherical regions correspond to water molecules spatially ordered by interaction with the ion and by hydrogen bonding. Thus the model is structural rather than continual. The relationship given by Bottcher for the interaction energy between an ion of charge, q , at a distance, s , from a single dielectric sphere of radius a is

$$-W = \frac{\epsilon - 1}{2} q^2 \sum_{l=0}^{\infty} \frac{l}{l+1} \frac{a^{2l+1}}{s^{2l+2}} \quad (2)$$

Here $a = r_w = 1.38 \text{ \AA}$, the radius of the water molecule as deduced from X-ray and electron diffraction data²⁰ on ice. The quantity $s = r_i + r_w$, where r_i is the ionic radius. In general $s = R(K)$ as discussed below. Equation 2 follows from a solution of Laplace's equation under appropriate boundary conditions.¹³ Note that the usual properties ascribed to solvent molecules, such as dipole or quadrupole moments, do not appear, but rather the general dielectric constant function. Clearly, ϵ will depend on the dipole moment, μ , and other molecular properties such as the Kirkwood correlation factor,²¹ g , which is closely related to the solvent structure. The dielectric constant in eq 2 also depends on the electric field strength.

The second building block in the model, eq 3, due to Booth^{21,22} provides the necessary expression for ϵ as a function of electric field strength and thus distance from the ion:

$$\epsilon = n^2 + \frac{28N_0\pi(n^2 + 2)\mu_v}{3(73)^{1/2}E} \left[\coth(x) - \frac{1}{x} \right] \quad (3)$$

where

$$x = \frac{73^{1/2} \mu_v (n^2 + 2) E}{6 kT}$$

and the term in brackets is the Langevin function. In eq 3 N_0 is the particle density of water (cm^{-3}); μ_v , the dipole moment according to Booth, is $2.1 \times 10^{-18} \text{ esu-cm}$; n is the optical refractive index; and E is the electric field strength in esu. Equation 3, which is based on Kirkwood's theory, contains Booth's approximate correlation factor derived from the hydrogen-bonded structure of water. Equation 3 has been used in several previous studies of hydration.⁴

The next step in assembling the theory was to generalize eq 2 and 3 so that ϵ and $-W$ could be calculated at the positions of the water molecules at various distances from the central ion. The field around an ion is a function of distance; therefore, we make the calculation of a "differential hydration energy" and then sum the results at each distance. This part of the calculation recognizes the discrete structure of liquid water (a hydrogen-bonded network) and is consistent with the familiar notion of various layers, shells, or spheres of hydration, i.e., primary, secondary, and so forth. Using this method we calculated the contribution to $\Delta G_{\text{hyd}}(\text{el})$ of various shells of water molecules as a function of distance. Then the contributions from each shell at a certain distance are summed to give the final result for the electrostatic contribution.

The input to the computer program consisted of Z , the integral charge on the ion; N , the number of water molecules in the primary hydration layer; and r_i , the crystal radius of the ion as given by Pauling.²³ Marcus¹ has concluded that the Pauling radius is a good measure of the size of solvated ion. He showed that a plot of crystal radius versus ion-water distances derived by a variety of methods including Monte Carlo, molecular dynamics, X-ray, and neutron diffraction gave a linear relation with unit slope and intercept of 1.39 \AA for the radius of the water molecule.

The formula (in \AA) for the distance between the central ion and the K th dielectric sphere is

$$R(K) = (r_i + 1.38) + 2.76K \quad (4)$$

where K was varied from 0 to 9. $K = 0$ corresponds to the first or inner hydration shell. The dielectric constant is given by $f\{E[R(K)]\}$, where f stands for Booth's eq 3. The computational task was to find $\epsilon[R(K)]$ at each of the K th shells of water molecules. This was accomplished by first assuming $\epsilon = 1$ and then calculating $E(K)$ as $Z^2/[R(K)\epsilon(K)]$. This first estimate of the field gave the second estimate of ϵ by means of eq 3 and thus a second estimate of the field at $R(K)$. This iterative process was performed until self-consistency was achieved at each $R(K)$. The criterion for terminating the calculation loop was that two consecutive $\epsilon(K)$ differed by less than 0.1%. The resulting value $\epsilon(K)$ was used in the first 10 terms in the summation over l in eq 2 to give the contribution to $\Delta G_{\text{hyd}}(\text{el})$ at that distance. The number of ions in the primary hydration shell ($K = 0$) is N as given in Table VII. At each distance beyond the first hydration shell, $K > 0$, the number of neighbors was assumed to be given by $N(K) = 2NK$.

This algorithm follows from the assumption that each water molecule in the primary shell can bind two additional water molecules by means of hydrogen bonding, thus forming the second shell. The molecular binding sites are either the two lone pairs of electrons on oxygen or the pair of hydrogen atoms. The number of neighbors in the third shell is similarly composed of the sum of the pairs of water molecules bound to each molecule in the second shell. The exact prescription for calculating the number of neighbors beyond the second shell is relatively unimportant because of the small energy contribution from far shells. In the calculations, the first 10 discrete distances of water spheres from the central ion were included to estimate the energetic contribution of the roughly first 30 \AA of water around the infinitely dilute ion. This means that 10 spheres of hydration were calculated. Following Buckingham,^{8,10} the hard-sphere model was assumed for the repulsive energy.

Quantum Mechanical Dispersion Energies. The chemical free energy of hydration, ΔG_{hyd} , was calculated by adding the dispersion

(17) (a) Bucher, M.; Porter, T. L. *J. Phys. Chem.* **1986**, *90*, 3406. (b) Bucher, M. *J. Phys. Chem.* **1986**, *90*, 3411.

(18) Bockris, J. O'M.; Hill, T. L. *Electrochim. Acta* **1964**, *9*, 347.

(19) Bockris, J. O'M.; Swinkels, D. A. J. *J. Electrochem. Soc.* **1964**, *111*, 736.

(20) Eisenberg, D.; Kauzman, W. *The Structure and Properties of Water*; Oxford University Press: Oxford, 1969; p 74.

(21) Booth, F. *J. Chem. Phys.* **1951**, *19*, 391.

(22) Booth, F. *J. Chem. Phys.* **1951**, *19*, 1327.

(23) Pauling, L. *The Nature of the Chemical Bond*, 3rd ed.; Cornell University Press: Ithaca, NY, 1960; Chapter 13.

TABLE I: Results for Na⁺

$R(K), \text{\AA}$	$E, \text{esu/cm}$	ϵ	$(\cos \theta)$	$-W(K), \text{eV}$
2.33	36200	23.2	0.903	3.512
5.09	2266	81.8	0.200	0.235
27.17	77	83.8	0.007	0.001
				3.858 ^a

^a $-\Delta G_{\text{hyd}}(\text{el})$.TABLE II: Results for Rb⁺

$R(K), \text{\AA}$	$E, \text{esu/cm}$	ϵ	$(\cos \theta)$	$-W(K), \text{eV}$
2.86	9669	60.7	0.630	2.462
5.62	1843	82.4	0.164	0.273
27.7	75	83.8	0.007	0.002
				2.891 ^a

^a $-\Delta G_{\text{hyd}}(\text{el})$.TABLE III: Results for F⁻

$R(K), \text{\AA}$	$E, \text{esu/cm}$	ϵ	$(\cos \theta)$	$-W(K), \text{eV}$
2.74	11530	55.5	0.684	3.419
5.50	1928	82.4	0.171	0.341
27.58	75	83.8	0.006	0.002
				3.947 ^a

^a $-\Delta G_{\text{hyd}}(\text{el})$.TABLE IV: Results for Fe²⁺

$R(K), \text{\AA}$	$E, \text{esu/cm}$	ϵ	$(\cos \theta)$	$-W(K), \text{eV}$
2.14	677000	3.10	0.994	16.086
4.9	5409	73.9	0.431	1.644
7.66	1990	82.3	0.177	0.394
26.98	157	83.8	0.014	0.008
				18.452 ^a

^a $-\Delta G_{\text{hyd}}(\text{el})$.

energies to the classical electrostatic energy, $\Delta G_{\text{hyd}}(\text{el})$, outlined above. We followed the discussion of Pitzer¹⁶ and employed the Kirkwood-Müller dispersion energy formula, eq 5, for a pair of particles A and B.

$$U_{\text{disp}} = -\frac{6mc^2\alpha_A\alpha_B}{N_0R^6} \left[\frac{\alpha_A}{\chi_A} + \frac{\alpha_B}{\chi_B} \right]^{-1} \quad (5)$$

The dispersion energy depends on the sixth power of the separation, the electronic polarizability, α , and diamagnetic susceptibility, χ , of the particles. The appropriate physical constants have been tabulated¹⁶ for each inert gas configuration. We assumed that the ion-water dispersion interaction could be represented by the appropriate inert gas-neon interaction. The neon properties were chosen to represent the water molecule because most of the electron density in the molecule resides on the oxygen atom. Inserting the physical constants and using Ne properties to represent the water molecule, we obtain eq 6, expressed in kcal mol⁻¹

$$U_{\text{disp}} = -\frac{46.92N\alpha_B}{R^6} \left[0.0555 + \frac{\alpha_B}{\chi_B} \right]^{-1} \quad (6)$$

where B represents any solvated ion. In eq 6, distance is expressed in angstroms, polarizability is expressed in 10⁻²⁴ cm³, susceptibility is expressed in 10⁻⁶ cm³, and N is the number of water molecules in the primary hydration sphere. The ratio of the magnetic susceptibility to the polarizability for the ions was calculated from the appropriate inert gas values.¹⁶ If the ion did not have an inert gas configuration, interpolated or extrapolated (in the case of transition-like ions) values were employed. For example, the properties of Fe²⁺ were interpolated between the values for Kr and Ar according to the number of electrons.

Pauling crystal radii for certain transition-metal ions were assumed to reflect the crystal field stabilization energy (crystal bond shortening), and therefore no crystal field energies were

TABLE V: Results for Fe³⁺

$R(K), \text{\AA}$	$E, \text{esu/cm}$	ϵ	$(\cos \theta)$	$-W(K), \text{eV}$
2.02	1486000	2.38	0.997	38.887
4.78	11170	56.5	0.675	4.054
7.54	3168	80.0	0.274	0.945
26.86	238	83.8	0.021	0.018
				44.652 ^a

^a $-\Delta G_{\text{hyd}}(\text{el})$.TABLE VI: Results for Ce⁴⁺

$R(K), \text{\AA}$	$E, \text{esu/cm}$	ϵ	$(\cos \theta)$	$-W(K), \text{eV}$
2.39	1391000	2.42	0.997	46.894
5.15	15960	45.4	0.769	8.693
7.91	3928	78.2	0.331	2.303
10.67	2054	82.2	0.182	0.916
27.23	309	83.8	0.028	0.053
				59.911 ^a

^a $-\Delta G_{\text{hyd}}(\text{el})$.TABLE VII: Comparison of Calculated and Observed Chemical Free Energies of Hydration of Gaseous Ions at 25 °C (kcal mol⁻¹)^a

ion	$r_c, \text{\AA}$	N	$-\Delta G_{\text{disp}}$	$-\Delta G_{\text{hyd}}(\text{calcd})$	$-\Delta G_{\text{hyd}}^b$	$-\Delta G_{\text{hyd}}^c$
H ⁺	0.392 ^d	4	0	(260.1)	260.5	259.2
Li ⁺	0.78	4	3.9	119.6	123.5	120.8
Na ⁺	0.95	4	4.3	93.2	98.3	97.0
Ag ⁺	1.26	8	2.0	108	114.5	113
K ⁺	1.33	6	5.5	77.0	80.8	79.3
Rb ⁺	1.46	7	9.1	75.8	76.6	74.2
Cs ⁺	1.69	8	12	69.2	71.0	66.5
F ⁻	1.36	8	3.2	94.2	103.8	88.2
OH ⁻	1.40 ^e	8	2.9	88.6	90.6	
Cl ⁻	1.81	12	6.2	79.9	75.8	74.8
Br ⁻	1.95	12	7.1	69.4	72.5	67.9
I ⁻	2.16	12	7.7	57.1	61.4	59.0
Mg ²⁺	0.64	5	12	454	455	453
Cu ²⁺	0.72	6	38	497	499	495
Zn ²⁺	0.74	6	44	486	485	482
Fe ²⁺	0.76	6	42	467	456	450
Ca ²⁺	0.99	7	21	365	381	378
Cd ²⁺	0.97	8	39	443	431	428
Hg ²⁺	1.10	9	60	443		434
Pb ²⁺	1.20	8	53	355	358	355
Ba ²⁺	1.35	9	27	318	315	313
Al ³⁺	0.50	4	15	997	1103	1099
Fe ³⁺	0.64	6	49	1079	1036	1032
Cr ³⁺	0.69	6	53	1077	1037	1036
Eu ³⁺	1.03	9	59	815	843	851
Ce ³⁺	1.11	10	53	805	804	808
La ³⁺	1.15	10	48	761	791	777
Ce ⁴⁺	1.01	10	68	1448		1471 ^f

^a r_c is the Pauling crystal radius. N is the primary hydration number. $-\Delta G_{\text{hyd}}(\text{calcd})$ is the sum of $-\Delta G_{\text{hyd}}(\text{el})$ and $-\Delta G_{\text{disp}}$. Chemical free energies means that the small energy change associated with the potential drop across the vacuum-solvent interface is not included in the hydration free energies in this paper. ^b Reference 4, experimental values. ^c Reference 1, experimental values. ^d Empirical radius to give to -260.1 kcal mol⁻¹. ^e Thermochemical radius, ref 24. ^f Data from ref 24 and 43.

added to the calculated hydration energies.

Results and Discussion

Typical results for the dielectric constant and hydration energy as a function of field and distance are given in Tables I-VI for various ions. The calculated average cosine of the angle between the field and the water dipole is also given. These values show the range of influence of the electric field of the ion. For singly charged ions, $(\cos \theta)$ falls to 0.1 at 8-10 Å and 10-15 Å for +3 or +4 species. The free energy value at the bottom of the last row represents the summation of $-W = \Delta G_{\text{hyd}}(\text{el})$ at each distance.

The Gibbs free energies of hydration, given in the fourth column of Table VII, were obtained by adding the dispersion energies (column 7) to $\Delta G_{\text{hyd}}(\text{el})$. Columns 5 and 6 contain experimentally

derived values. In general the overall agreement is very good. Note that the effective radius of the proton, 0.392 Å, is the value required to obtain agreement with experiment, assuming $N = 4$. Note that Bucher and Porter¹⁷ found 0.35 Å by a different type of electrostatic calculation. The OH⁻ radius, 1.40 Å, is the thermochemical radius²⁴ used in lattice energy calculations. We used Pauling crystal radii for all other ions with the exception of Li⁺ for which the Goldschmidt value,^{1,23} 0.78 Å, was used. The inapplicability of the standard Pauling radius, 0.60 Å, can be explained by analogy to the situation in Li⁺ salts. Due to the small size of the Li⁺ ion, the anion-anion contact repulsions play a critical role in keeping the lithium-anion distance¹ greater than the sum of the standard Pauling radii. By analogy, intermolecular water molecule repulsions are operational in the primary solvation shell causing a similar effect. We are not aware of any accurate value for the free energy of hydration of S²⁻; therefore sulfide ion was not included.

The average percent deviations between the calculated and experimentally derived results for each charge are the following: -1, 3.5%; +1, 2.5%; +2, 1.7%; +3, 1.5%. In the single +4 case of Ce⁴⁺, the deviation was 1.5%. The calculated results are proportional to N , the primary hydration number. This means that increasing or decreasing the N value by 1 would lead to a relative deviation in the calculated ΔG_{hyd} of (100/ N)%. The relative error is 25% for $N = 4$ and 12% for $N = 12$. This deviation is larger than the experimental uncertainty in ΔG_{hyd} , and therefore the integral hydration numbers are unique within the model.

Primary Hydration Numbers. A large body of data on hydration numbers is presented in the review by Hinton and Amis.²⁵ A well-known difficulty is that of finding agreement among the various experimental methods for deriving hydration numbers. We decided against detailed comparison of our N values to those in the review²⁵ because of the ambiguity in the literature. This should not be taken to mean that our N values are unreasonable. Certainly, we could justify most, if not all, of our N values by quoting results obtained by several different methods. But, it is doubtful that a single method would yield results consistent with ours for all ions. Indeed no single method has been applied to all the ions in Table VII.

Some of the reasons for the difficulties one encounters are the following. A number of methods depend on assignment of a standard hydration number to a reference ion. We found it difficult to find a set of results that gave both a reference value and the sought-for value consistent with our results. Different methods do not even agree on whether the hydration number should increase or decrease with the size of the ion. For example, Conway⁷ has noted that primary hydration numbers determined by nuclear magnetic resonance^{26,27} increase with ionic radius whereas values derived from other methods including mobility²⁵ indicate smaller hydration numbers for larger ions. To compare our N values, one must select a method that measures the primary hydration sphere. This generally means NMR and X-ray diffraction²⁸ methods in concentrated electrolytes. Experimental²⁹ and theoretical³⁰ evidence indicates that apparent hydration numbers decrease with increasing salt concentration. Our model and most model calculations to date apply to infinite dilution. Further, there is evidence³¹ that, in concentrated solutions, the primary hydration number depends on the identity of the counterion.

The clear trend in our results is that primary hydration numbers increase with the size of the ion. Studies that have indicated larger primary hydration numbers for larger ions include NMR,^{26,27} molecular dynamics³⁰⁻³³ and ab initio quantum¹⁴ calculations, and

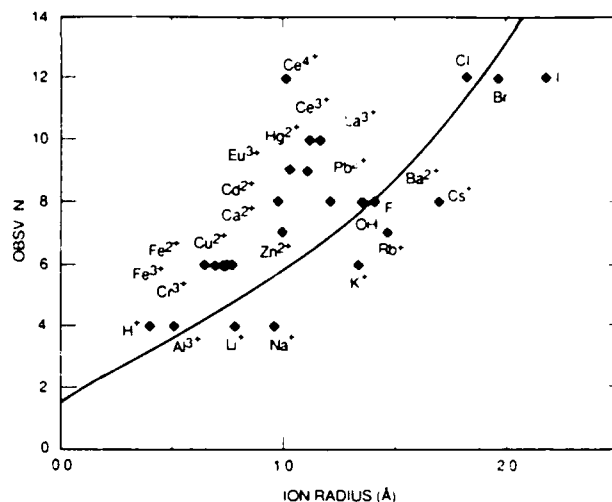


Figure 1. Observed ligancy in oxides (solid line) and inner-sphere hydration numbers found in this work versus Pauling crystal radius.

X-ray diffraction.²⁸ By analogy to ligancy trends in crystalline solids, we might expect larger primary hydration numbers for larger ions. The actual number of ligands in the solid state is mainly determined by radius ratio effects.²³

We looked for a correlation between our N values and the number of nearest neighbors expected on the basis of crystal packing. The analogy between frozen water in the primary hydration shell and solid-state water, ice, has been made before. Oxides were chosen for comparison, and Pauling²³ has tabulated the expected and observed ligancies as a function of ionic radius. The observed values versus the known ligancy are represented by the solid line in Figure 1. The points represent the values of N (Table VII) found in the present calculations. It is seen that the observed ligancies in the solid state and in the highly polarized liquid state in the inner hydration layer correlate well, especially for univalent ions. Our N values are integers, again in analogy to solid-state ligancy and in contrast to many fractional experimental determinations.²⁵ There is little controversy concerning the primary hydration number of four²⁵ for H⁺, Li⁺, and Na⁺. The $N = 4$ for Al³⁺ does not agree with the commonly accepted value³⁴ of 6. The transition elements Fe²⁺, Fe³⁺, Zn²⁺, and Cu²⁺ were required to be hexaquo complexes³⁵ to obtain agreement with experimental hydration energies. We found nine inner-layer water molecules for Eu³⁺; a value of eight or nine is supported by spectroscopic^{36,37} evidence. The value of ten for the three other lanthanides³⁸ in Table VII is very reasonable given the rather confident value of nine for Eu³⁺.

The most unconventional result is $N = 12$ for the halogens Br⁻, Cl⁻, and I⁻. Such large numbers are consistent with the icosahedral arrangement,^{23,39} which represents the largest number of spherical particles that can be packed around an isodimensional central sphere. As a group, these halogen ion values fall very close to the solid-state-ligancy line in Figure 1, yet hydration numbers between 4 and 0 have been reported.²⁵ The following values have been determined for F⁻, Cl⁻, Br⁻, and I⁻ by the NMR method²⁶ and based on $N = 6$ for K⁺; $N = 9.9, 13.2, 16.2$, and 21.8, respectively. Unfortunately, $N = 1$ was found for Li⁺ in the same investigation. Molecular dynamics calculations³¹ give $N = 8-9$ for Cl⁻ in 2.2 M CsCl. X-ray diffraction values²⁸ for the inner layer range from 6 to 9 and may depend on concentration. These results support our large inner-sphere solvation numbers and at

(24) Smith, D. J. *Chem. Educ.* 1977, 54, 540.

(25) Hinton, J. F.; Amis, E. S. *Chem. Rev.* 1971, 71, 627.

(26) Fabricand, B. P.; Goldberg, S. S.; Leifer, R.; Ungar, S. G. *J. Chem. Phys.* 1961, 34, 425.

(27) Swift, T. J.; Sayre, W. G. *J. Chem. Phys.* 1966, 44, 3567.

(28) Lawrence, R. M.; Kruh, R. F. *J. Chem. Phys.* 1967, 47, 4758.

(29) Bockris, J. O'M.; Saluja, P. P. *J. Phys. Chem.* 1972, 76, 2140.

(30) Vogel, P. C.; Heinzinger, K. Z. *Naturforsch.* 1976, 31a, 476.

(31) Vogel, P. C.; Heinzinger, K. Z. *Naturforsch.* 1975, 30a, 789.

(32) Heinzinger, K.; Vogel, P. C. Z. *Naturforsch.* 1974, 29a, 1164.

(33) Heinzinger, K.; Vogel, P. C. Z. *Naturforsch.* 1976, 31a, 463.

(34) Akitt, J. W. *Faraday Discuss. Chem. Soc.* 1977, No. 64, 132.

(35) Cotton, F. A.; Wilkinson, G. *Advanced Organic Chemistry*, 3rd ed.; Interscience: New York, 1972; Chapter 21.

(36) Miller, D. G. *J. Am. Chem. Soc.* 1958, 80, 3576.

(37) Rossotti, F. J. *Faraday Discuss. Chem. Soc.* 1977, No. 64, 138.

(38) Reference 1, p 118.

(39) Reference 35, p 22.

TABLE VIII: Comparison of Inner-Sphere Free Energies of Hydration of Gaseous Ions at 25 °C (kcal mol⁻¹)

ion	<i>N</i>	$-\Delta G_{\text{calcd}}^{\text{inner}}^a$	$-(\Delta H - T\Delta S)^b$	$-\Delta G_{\text{calcd}}^c$	$-\Delta G_{\text{BC}}^d$
H ⁺	4	248	231	260.1	52
Li ⁺	4	111	92	119.6	46
Na ⁺	4	85	78	93.2	44
K ⁺	6	68	73	77.0	40
F ⁻	8	82	86	94.2	40
OH ⁻	8	76	86	88.6	39

^a Results of this work, including dispersion energy; see Table I and VII for examples. ^b Enthalpy from either Hartree-Fock (H-F) calculations (ref 14) or experimental data on gas-phase cluster reactions (ref 41 and 42). Total ΔS of hydration (ref 5). See text for further explanation. ^c Total calculated Gibbs energy of hydration, Table VII. ^d Gibbs energy of hydration for outer sphere calculated using eq 1a. Ionic radii from Table VII; $r_w = 1.38$ Å.

the same time point out the state of confusion about primary hydration numbers.

Inner- and Outer-Layer Gibbs Energy of Hydration. We define the inner (primary) hydration layer to include the *N* water molecules assumed to be in closest contact with the ion. The outer hydration sphere includes water molecules beyond the primary sphere. These definitions are similar to those employed in theories⁴⁰ of electron-transfer rates. It is frequently assumed^{8,10} that the outer hydration free energy of the ion-primary water complex is described by the Born model, eq 1a. The radius of this ion is given by the crystal radius of the ion plus 2.76 Å, the diameter of a water molecule. Using the results in Tables I-VI, we can determine, according to our calculations, how much of $\Delta G_{\text{hyd}}(\text{el})$ is attributed to ion-water interactions outside the primary sphere. For example, the calculated electrostatic interaction energy of $\text{Na}(\text{H}_2\text{O})_4^+$ with the remaining solvent is $3.86 - 3.51 = 0.35$ eV. Therefore 90% of the hydration energy of the Na⁺ resides in the inner layer. Similar figures for F⁻, Fe³⁺, and Ce⁴⁺ are 86, 87, 87, and 78%, respectively. The smaller percentage for Ce⁴⁺ results from the larger contribution, 14%, from the secondary hydration sphere. Application of the Born model to the $\text{Na}(\text{H}_2\text{O})_4^+$ complex ion gives $\Delta G_{\text{hyd}}(\text{outer}) = 1.83$ eV, a value 5 times larger than found in the present calculations. Such a discrepancy clearly signifies a major fault in one of the models.

Our calculations show that 78–90% of the electrostatic energy arises in the primary hydration sphere and that application of the Born model gives a large overestimation of the hydration energy of the ion-primary water complex. This result is not expected from previous electrostatic models.^{4,5,8–10}

The conclusion that most of the hydration energy resides in the inner layer follows from both quantum mechanical calculations and experimental energetics of ion-water cluster reactions. Table VIII shows data that support our results. The third column gives our calculated Gibbs energy of hydration for the inner-layer complex ion including the dispersion energies. The appropriate values for Na⁺, for example, may be obtained from Tables I and VII. As noted above, these numbers represent 80–90% of the total energy. The fourth column in Table VIII contains an approximation to the same Gibbs energy based on the *ab initio* Hartree-Fock (H-F) calculations¹⁴ or the experimental cluster enthalpies^{41,42} as follows. The experimental cluster enthalpy for $\text{H}(\text{H}_2\text{O})_4^+$ was used. For $\text{Li}(\text{H}_2\text{O})_4^+$, $\text{Na}(\text{H}_2\text{O})_4^+$, and $\text{K}(\text{H}_2\text{O})_6^+$, the H-F results were used; these were in close agreement¹⁴ with the experimental cluster enthalpies. In the case of $\text{F}(\text{H}_2\text{O})_8^-$, the H-F results for $\text{F}(\text{H}_2\text{O})_5^-$ were supplemented for the sixth to eighth water molecules by extrapolation of the H-F energy vs *N* plots (see Figure 13, ref 14). The result was an additional stabilization of 14 kcal mol⁻¹ for the water molecules 6–8. The

enthalpy data for $\text{OH}(\text{H}_2\text{O})_8^-$ were obtained by also adding 14 kcal mol⁻¹ to the experimental cluster enthalpy⁴¹ of $\text{OH}(\text{H}_2\text{O})_5^-$. The similar treatment of solvated F⁻ and OH⁻ is justified because they are isoelectronic.

In all cases, the total observed entropy⁵ of hydration of the gaseous ion was added to the H-F or cluster enthalpy on the assumption that all the entropy change is attributable to inner layer. This procedure makes the Gibbs energies in column 4 uncertain by several kcal mol⁻¹, because most, but not all, the entropy change is attributable to the inner layer.

The last column in Table VIII gives the Born contribution to the Gibbs energy of hydration, eq 1a, for the inner-layer complex of the ion and *N* water molecules. The agreement between columns 3 and 4 of Table VIII gives strong support to the calculation method based on our eq 2 and 3 above and the fact that inner-layer solvation dominates by far. The difference, column 5 minus column 3, is seen to be small compared to the Born charging term. This supports the conclusion that the energetic contributions to the hydration energy beyond the inner layer are much smaller than eq 1a would lead one to believe.

As stated by Bottcher,¹³ the simple expressions, like eq 1b,c, used in the description of the inner hydration layer, underestimate the interaction energy by 50–100%. These equations are based on conducting, point ion models, which are not valid at distances such that the radius of the particles is of the order of their separation. If this is correct, it would explain how the Born model, eq 1a, in combination with eq 1b,c for solvation of the ion-primary water complex was perceived to give accurate results. The underestimation of the Gibbs energy of hydration in the inner layer is canceled by the overestimation in the outer region (outside the first shell of water), and the sum of the energy in the two regions is approximately correct, at least for univalent ions.

These observations may have some bearing on the activation process for homogeneous and heterogeneous electron transfers to solvated ions. There has been disagreement concerning the relative importance of inner- and outer-sphere (-layer) contributions to the activation energy. According to Bockris and Kahn,⁴⁰ the outer-sphere activation would require simultaneous participation of a large number of solvent molecules, each having a small contribution to the activation energy. It is stated that this simultaneous activation is highly improbable. The reorganization of the equilibrium solvation coordinates is generally held to be the rate-determining step in the electron transfer. Our results suggest that the solvation energy resides mainly in the inner hydration layer, at least in the ideal solution state. This may mean that the reorganization process involves a relatively few solvent molecules, the order of *N* in Table VII. The contribution of each ion-solvent "bond" in an exchange reaction⁴² would then be the order of $\lambda/4N$, where λ is the observed reorganization energy. The change in inner-layer hydration with concentration and counterion mentioned above may be seen in the kinetics of electron transfer.

Summary. The Gibbs hydration energy has been calculated for 30 ions with -1 to +4 charge with typical deviations of 2% from the experimentally derived values. The inapplicable Born-type equations and other simple electrostatic functions were replaced by a more accurate series solution to the electrostatic problem of the interaction of an ion and a dielectric sphere. The classical electrostatic part of the calculation involves only the dielectric constant and discrete structure information. Quantum mechanical dispersion energies were added. Primary hydration numbers were chosen to give agreement between calculated and experimentally derived hydration energies. Small integer values ranging from 4 to 12 were obtained. These values, especially the smaller ones, are unique to the model. Pauling ionic radii were employed, except for the Li⁺, where ligand repulsions are probably operational and the empirical Goldschmidt value gives much better results. The resulting primary hydration numbers were correlated with the ionic radius as may be expected from known ligancy-size trends in solid-state chemistry. The calculations suggest that not only does the Born model not generally describe the primary solvation shell but also it does not hold for the solvation energetics

(40) Kahn, S. U. M.; Bockris, J. O'M. *The Chemistry and Physics of Electrocatalysis*; McIntyre, J. D. E., Weaver, M. J., Yeager, E. B., Eds.; Proceedings—Electrochemical Society 84; The Electrochemical Society: Pennington, NJ, 1984 (see also discussion of this paper by R. A. Marcus).

(41) Arshadi, M.; Kebabian, P. *J. Phys. Chem.* 1970, 74, 1466, 1483.

(42) Kebabian, P.; Sears, S. K.; Zolla, A.; Scarborough, J.; Arshadi, M. *J. Am. Chem. Soc.* 1967, 89, 6393.

(43) Powell, R. E.; Latimer, W. M. *J. Chem. Phys.* 1951, 19, 1139.

of the complex ion formed by the central ion and the primary hydration shell.

Acknowledgment. This work was supported by the Chemistry Division of the Office of Naval Research.

Registry No. H⁺, 12586-59-3; Li⁺, 17341-24-1; Na⁺, 17341-25-2;

Ag⁺, 14701-21-4; K⁺, 24203-36-9; Rb⁺, 22537-38-8; Cs⁺, 18459-37-5; F⁻, 16984-48-8; OH⁻, 14280-30-9; Cl⁻, 16887-00-6; Br⁻, 24959-67-9; I⁻, 20461-54-5; Mg²⁺, 22537-22-0; Cu²⁺, 15158-11-9; Zn²⁺, 23713-49-7; Fe²⁺, 15438-31-0; Ca²⁺, 14127-61-8; Cd²⁺, 22537-48-0; Hg²⁺, 14302-87-5; Pb²⁺, 14280-50-3; Ba²⁺, 22541-12-4; Al³⁺, 22537-23-1; Fe³⁺, 20074-52-6; Cr³⁺, 16065-83-1; Eu³⁺, 22541-18-0; Ce³⁺, 18923-26-7; La³⁺, 16096-89-2; Ce⁴⁺, 16065-90-0.